

Probabilistic energy forecasting through quantile regression in reproducing kernel Hilbert spaces

Luca Pernigo
luca.pernigo@usi.ch
Euler Institute, USI
Lugano, Switzerland

Rohan Sen
rohan.sen@usi.ch
Euler Institute, USI
Lugano, Switzerland

Davide Baroli
davide.baroli@usi.ch
Euler Institute, USI
Lugano, Switzerland

ABSTRACT

Accurate energy demand forecasting is crucial for sustainable and resilient energy development. To meet the Net Zero Representative Concentration Pathways (RCP) 4.5 scenario in the DACH countries, increased renewable energy production, energy storage, and reduced commercial building consumption are needed. This scenario's success depends on hydroelectric capacity and climatic factors. Informed decisions require quantifying uncertainty in forecasts. This study explores a nonparametric method based on *reproducing kernel Hilbert spaces* (RKHS), known as kernel quantile regression, for energy prediction. Our experiments demonstrate its reliability and sharpness, and we benchmark it against state-of-the-art methods in load and price forecasting for the DACH region. We offer our implementation in conjunction with additional scripts to ensure the reproducibility of our research.

CCS CONCEPTS

• **Mathematics of computing** → **Nonparametric statistics**; • **Computing methodologies** → **Feature selection**; • **Software and its engineering** → **Software libraries and repositories**.

KEYWORDS

Kernel method, quantile regression, energy forecast, probabilistic forecast, climate, GEFCom, SP2050, DACH

ACM Reference Format:

Luca Pernigo, Rohan Sen, and Davide Baroli. 2024. Probabilistic energy forecasting through quantile regression in reproducing kernel Hilbert spaces. In . ACM, New York, NY, USA, 13 pages. <https://doi.org/10.1145/nnnnnnn.nnnnnnn>

1 INTRODUCTION

Climate shock and the penetration of renewable energy sources are pivotal issues in the modern energy system, particularly in the DACH region (comprising Germany, Austria, and Switzerland). Recently, the Swiss Federal Office of Energy has published a comprehensive analysis to assess how to secure and produce a cost-efficient energy supply in *Swiss Energy Strategy 2050* and *Energy Perspectives 2050+*. Recently, Switzerland also adopted the long-term goal

Permission to make digital or hard copies of all or part of this work for personal or classroom use is granted without fee provided that copies are not made or distributed for profit or commercial advantage and that copies bear this notice and the full citation on the first page. Copyrights for components of this work owned by others than the author(s) must be honored. Abstracting with credit is permitted. To copy otherwise, or republish, to post on servers or to redistribute to lists, requires prior specific permission and/or a fee. Request permissions from permissions@acm.org.
Conference'17, July 2017, Washington, DC, USA

© 2024 Copyright held by the owner/author(s). Publication rights licensed to ACM.
ACM ISBN 978-x-xxxx-xxxx-x/YY/MM
<https://doi.org/10.1145/nnnnnnn.nnnnnnn>

ACM SIGENERGY Energy Informatics Review

of climate neutrality, aiming to decrease its energy-building consumption and deploy more renewable energy technologies. In addition to being essential to mitigate climate change, the performance of renewable energy sources and the demand for building energy depend on weather data and energy storage.

Within the SURE SWEET energy initiative, supported by the SFOE, the development of future sustainable and robust systems is corroborated by techno-economic models that predict long-term scenarios and pathways, which are resilient to climate shocks [Panos et al. 2023]. These models require a large amount of technical and economic data and their quality influences the reliability of the results, for example, bottom-up techno-economics model [Kannan 2018], which provides hourly prediction, EXPANSE [Trutnevtey 2013], building stock model [Nägeli et al. 2020], macro-economics GEM-3M and life cycle assessment [Luh et al. 2023]. The projection of these models is affected by weather data. For example, the Swiss building stock model designs decarbonisation pathways for different buildings' archetypes, whose isolation and heating performance vary with external temperature. As a result, the prediction of hourly loads by transmission system operators is influenced by the variability and uncertainty of climate factors and is dependent on many parameters of the techno-economics models.

In particular, the pathways predicted by SURE models to achieve the Swiss net-zero scenario in conjunction with the RCP pathway 4.5 address the primary issue of reliable energy supply. This is essential because it requires an increase in renewable energy sources to meet annual net electricity demand of 80–100 TWh by 2050, compared to the current 60 TWh SFOE 2022b. One of the factors of such an increase in electricity due to sustainable mobility is up to 22 TWh [Kannan et al. 2022]. To guarantee uninterrupted energy supply, even under extreme weather conditions [Ho-Tran and Fiedler 2024], in SFOE 2022a various scenarios have been examined: dependence on importing electricity from the European market and expansion of technologies that can provide or save electricity in winter, for example wind, alpine photovoltaic, seasonal heat storage or nuclear power.

In such energy scenarios, forecasting models are needed to provide reliable energy management and probabilistic projections of socio-economical energy technologies [Zielonka et al. 2023]. In addition, these models serve as a decision support tool for the transmission system operator (TSO), such as SwissegGrid, to determine the balance of reserves [Abbaspourtorbati and Zima 2016] and for policy-makers to develop a transition to sustainable energy sources. Due to the challenges described above, this work aims to investigate probabilistic forecasting to assess the uncertainty of energy supply

due to fluctuations in hydroelectric capacity at day frequency, meteorological, and the intermittency of renewable energy sources at high temporal frequency, i.e., at hour resolution.

In electricity forecasting state-of-the-art research, the focus has been mostly on point-forecast methods, that is, methods that output a single value for each target timestamp. Point forecasts are usually assessed using well-known criteria such as the *root mean squared error (RMSE)* and the *mean absolute error (MAE)*. Lately, the electricity forecasting community is shifting towards the probabilistic forecasting framework. The advantage of these methods is that they are more informative than a single-point prediction. [Gneiting et al. 2007] introduces how to assess the quality of probabilistic forecasts by maximizing the sharpness of prediction distributions under calibration constraints. Calibration refers to the statistical consistency between the predicted distributions and the observations, while sharpness refers to the spread of the forecast distributions. Scoring rules assign numerical scores to the forecasts based on the predicted distribution and the value that is materialized. In the assessment of the probabilistic model, the most widely used scores are pinball loss and the *continuous ranked probability score (CRPS)*. [Gneiting 2011] studies the class of loss functions that lead to optimal predictors for the quantiles of a predictive distribution.

Probabilistic forecasting is gradually becoming an active research area for academia, where different researchers propose parametric and non-parametric models for forecasting specific outputs: wind, solar [Gneiting et al. 2023], prices [Nowotarski and Weron 2018a] or demand [Phipps et al. 2023]. A tutorial review on probabilistic load forecasting by [Hong et al. 2016] covers forecasting techniques, auxiliary methodologies, evaluation metrics, and good sources of reference. Another review paper by [Nowotarski and Weron 2018a] presents measures, tests, and guidelines for the rigorous use of probabilistic electricity forecasting methods. Another study, see [Van der Meer et al. 2018], provides a broad overview of probabilistic forecasting, specifically, the authors focus on solar power and load forecasting. In [Ziel and Steinert 2018] an extensive literature review has been carried out by classifying electricity price forecasting papers according to various attributes such as prediction horizon, data used, predictors, accuracy measures, and models proposed.

This article addresses probabilistic forecasting by adopting the *kernel quantile regression (KQR)* method within the RKHS framework. This method was introduced in [Takeuchi et al. 2006] and further investigated in [Li et al. 2007; Sangnier et al. 2016; Zhang et al. 2016; Zheng 2021]. The method offers a non-parametric and non-linear way to provide probabilistic forecasts. The main contribution of this article is to perform a probabilistic forecast with KQR for Swiss, Austrian, and German energy systems, where the data are extracted from [ENTSO-E Transparency Platform](#), [SECURES-Met](#) [Formayer et al. 2023] and [C3S Energy](#)[Dubus et al. 2023], which is designed to assess the impacts of climate variability and climate change on the energy sector. The probabilistic forecast with KQR has also been validated in the GEFCom test case, where our Python-based open-source implementation compares favourably with the top teams in the probabilistic forecast of electricity load and price.

Kernel quantile regression has received little attention in the energy forecasting literature. [He and Li 2018] employs it to forecast wind power generation and compares it to a quantile regression

neural network. [Moreira et al. 2016] uses it to forecast electricity prices for the Iberian electricity market. In that study, kernel quantile regression is compared with linear quantile regression, neural network quantile regression, random forest, and regression boosting. [He et al. 2017] studies the choice of kernel functions in the context of short-term load forecasting. However, no research has yet been done that thoroughly compares KQR to other state-of-the-art methods in the specific context of medium-term electricity load forecasting. Therefore, our second contribution is applying kernel quantile regression to the medium load forecasting setting, see section 4, sticking to best practices and guidelines of popular literature reviews in the field of probabilistic electric load forecasting (PLF) [Hong and Fan 2016; Lago et al. 2021; Nowotarski and Weron 2018b]. We implemented our version of KQR since there were no implemented Python packages available. We made our model class inherit from the scikit template classes `BaseEstimator` and `RegressorMixin`; by doing so, our KQR is compatible with useful scikit learn functionalities such as grid search, cross-validation, and metric scorers; that is, our method is compatible with the scikit-learn API, see [Pedregosa et al. 2011]. Sharing our implementation with the research community is the last contribution of this paper.

1.1 Outline

The rest of this article is structured as follows. In Section 2, we review quantile regression, in particular, kernel quantile regression. In Section 3, KQR is benchmarked against other popular quantile regression models on data extracted from [ENTSO-E Transparency Platform](#). Following, a kernel wise comparison is carried out on the [SECURES-Met](#) data [Formayer et al. 2023]. Furthermore, we evaluate the performance of KQR in the context of the challenge GEFCom2014 in Section 4. Finally, in Section 5, we conclude the article.

2 KERNEL QUANTILE REGRESSION

We first briefly review quantile regression here and then cover the details regarding kernel quantile regression. *Quantile regression (QR)* is a method used in various fields, such as econometrics, social sciences, and ecology, to analyse the empirical distribution. Estimates a target quantile of the response variable y based on a predictor vector, \mathbf{x} . QR is more robust to outliers in the data compared to the usual least-squares regression. It is also suitable for cases where there is heteroscedasticity in the errors. Additionally, using a series of quantile values provides a better description of the entire distribution than a single value, such as the mean. [Koenker and Bassett Jr 1978] showed that the *pinball loss* function

$$\rho_q(u) = \begin{cases} qu & \text{if } u \geq 0, \\ -(1-q)u & \text{if } u < 0, \end{cases} \quad (2.1)$$

can recover a target quantile of interest, q where $0 \leq q \leq 1$. We refer the reader to Appendix A for further details on the same.

Given empirical samples $(\mathbf{x}_i, y_i)_{i=1}^n$, with $\mathbf{x}_i \in \mathbb{R}^d$, $y_i \in \mathbb{R}$, quantile regression [Koenker 2005; Koenker and Hallock 2001] seeks to estimate the q -th conditional quantile of the response variable y as a linear function of the explanatory variables \mathbf{x}_i by solving the

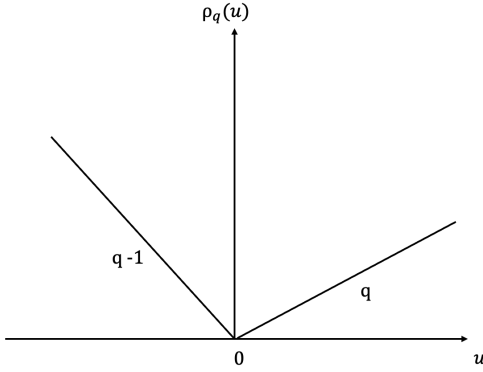


Figure 1: Pinball loss function at the q quantile—the lower the pinball loss, the more accurate the quantile forecast is.

following minimization problem

$$\operatorname{argmin}_{\beta \in \mathbb{R}^n} \sum_{i=1}^n \rho_q(y_i - \mathbf{x}_i^\top \beta). \quad (2.2)$$

With the motivation to perform QR that can also capture additional complexity and non-linearity in the data, several extensions of Problem 2.2 were explored in [Hwang and Shim 2005; Li et al. 2007; Takeuchi et al. 2006; Xu et al. 2015; Zhang et al. 2016]. In the above works, the authors investigated non-parametric versions of the QR, called the kernel quantile regression, which is based on the framework of reproducing kernel Hilbert spaces. The key idea of KQR is to first transform the data samples non-linearly to a potentially higher-dimensional space of functions \mathcal{H} via a feature map $\phi(\cdot)$, and then consider an affine function of the transformed data. Precisely, the conditional pinball loss of the response variable $\rho_q(y|\mathbf{x})$ given the predictor vector \mathbf{x} is approximated by functions of the form

$$f(\mathbf{x}) = \langle \mathbf{w}, \phi(\mathbf{x}) \rangle_{\mathcal{H}} + b, \quad (2.3)$$

where $\mathbf{w} \in \mathcal{H}$ is the regression coefficient and $b \in \mathbb{R}$ is the intercept term. In particular, the map $\mathbf{x} \mapsto \phi(\mathbf{x})$ is implicitly defined by a reproducing kernel \mathcal{K} that makes \mathcal{H} an RKHS, which can contain a sufficiently rich class of functions. We first give herein the definition of RKHS and refer the reader to [Berlinet and Thomas-Agnan 2011; Schölkopf and Smola 2018] for more details of the same.

Definition 2.1. Let $(\mathcal{H}, \langle \cdot, \cdot \rangle_{\mathcal{H}})$ be a Hilbert space of real-valued functions on $\mathcal{X} \subset \mathbb{R}^d$. A function $\mathcal{K} : \mathcal{X} \times \mathcal{X} \rightarrow \mathbb{R}$ is called a *reproducing kernel* of \mathcal{H} if and only if

$$\mathcal{K}(\mathbf{x}, \cdot) \in \mathcal{H} \quad \text{for all } \mathbf{x} \in \mathcal{X}; \quad (2.4)$$

$$\langle h, \mathcal{K}(\mathbf{x}, \cdot) \rangle_{\mathcal{H}} = h(\mathbf{x}) \quad \text{for all } h \in \mathcal{H}, \mathbf{x} \in \mathcal{X}. \quad (2.5)$$

If the above two properties hold, \mathcal{H} is called a *reproducing kernel Hilbert space*. Associated to every RKHS \mathcal{H} , there exists the canonical feature map [Aronszajn 1950] $\phi : \mathcal{X} \rightarrow \mathcal{H}, \mathbf{x} \mapsto \mathcal{K}(\mathbf{x}, \cdot)$ such that

$$\langle \phi(\mathbf{x}), \phi(\mathbf{x}') \rangle_{\mathcal{H}} = \mathcal{K}(\mathbf{x}, \mathbf{x}') \quad \text{for all } \mathbf{x}, \mathbf{x}' \in \mathcal{X}. \quad (2.6)$$

Furthermore, given a finite set of data samples $\{\mathbf{x}_1, \dots, \mathbf{x}_n\} \subset \mathcal{X}$, the *kernel matrix* defined as $\mathbf{K} := [\mathcal{K}(\mathbf{x}_i, \mathbf{x}_j)]_{i,j=1}^n \in \mathbb{R}^{n \times n}$ is a symmetric and positive semi-definite matrix.

ACM SIGENERGY Energy Informatics Review

In the context of KQR, [Li et al. 2007; Takeuchi et al. 2006; Zheng 2021] consider the following regularised objective function

$$R[f] := \frac{1}{m} \sum_{i=1}^m \rho_q(y_i - f(\mathbf{x}_i)) + \frac{\lambda}{2} \|\mathbf{w}\|_{\mathcal{H}}^2, \quad (2.7)$$

for $f(\mathbf{x}) = \langle \mathbf{w}, \phi(\mathbf{x}) \rangle_{\mathcal{H}} + b$, cp. (2.3), where $\mathbf{w} \in \mathcal{H}$ and $\lambda > 0$ is a hyper-parameter. The first term in (2.7) measures the empirical loss in terms of the pinball function, cp. Equation 2.1, and the second term measures the complexity of the model, see [Vapnik 1997]. In particular, [Li et al. 2007; Takeuchi et al. 2006; Zheng 2021] consider the following minimization problem

$$\operatorname{argmin}_{\mathbf{w} \in \mathcal{H}, b \in \mathbb{R}} C \sum_{i=1}^n \rho_q(y_i - (\langle \mathbf{w}, \phi(\mathbf{x}_i) \rangle_{\mathcal{H}} + b)) + \frac{1}{2} \|\mathbf{w}\|_{\mathcal{H}}^2, \quad (2.8)$$

where $C = \frac{1}{\lambda m} > 0$ is the factor that balances the model complexity and the total empirical pinball loss on the sample data. Using the representer theorem, see [Schölkopf et al. 2001], we have that the optimal solution to Problem 2.8 can be written as a linear combination of kernel functions evaluated at the training examples, i.e. it has the following form

$$\mathbf{w}^{\star} = \sum_{i=1}^n a_i^{\star} \phi(\mathbf{x}_i), \quad (2.9)$$

or equivalently,

$$f^{\star}(\mathbf{x}) = \sum_{i=1}^n a_i^{\star} \langle \phi(\mathbf{x}), \phi(\mathbf{x}_i) \rangle_{\mathcal{H}} + b = \sum_{i=1}^n a_i^{\star} \mathcal{K}(\mathbf{x}, \mathbf{x}_i) + b \quad (2.10)$$

The optimal coefficients a_i^{\star} , $1 \leq i \leq n$ are obtained via

$$\begin{aligned} \mathbf{a}^{\star} &= \operatorname{argmin}_{\mathbf{a} \in \mathbb{R}^n} \frac{1}{2} \mathbf{a}^\top \mathbf{K} \mathbf{a} - \mathbf{a}^\top \mathbf{y} \\ \text{s.t.} \quad & C(q-1)\mathbf{1} \leq \mathbf{a} \leq Cq\mathbf{1} \\ & \mathbf{a}^\top \mathbf{1} = 0, \end{aligned} \quad (2.11)$$

where $\mathbf{y} := [y_i]_{i=1}^n \in \mathbb{R}^n$, $\mathbf{1} := [1, \dots, 1]^\top \in \mathbb{R}^n$, and $\mathbf{K} \in \mathbb{R}^{n \times n}$ is the kernel matrix of the samples $(\mathbf{x}_i)_{i=1}^n$. We refer the reader to Appendix B for further details. Note that Problem 2.11 is a quadratic programming problem and, thus, can be solved by traditional solvers.

3 NUMERICAL EXAMPLES

All the numerical experiments have been performed in Python on a 3.2 GHz 16 GB Apple M1 Pro. Since KQR involves a quadratic programming problem, cp. (2.11), we used the interior-point method implemented in the cvxopt library to solve it. For a detailed description of cvxopt solvers and algorithms available, we refer the interested reader to the manual [Vandenberghe 2010]. All scripts are made publicly available at the [Github repository](#) along with the cleaned data.

3.1 Energy charts case study

In this case study, KQR is compared against popular quantile regressor models, the kernel of choice here is the Laplacian equipped with the Manhattan distance (Absolute Laplacian). The dataset for this case study comes from [Energy charts](#) which retrieves data from

Volume 4 Issue 4, October 2024

the [ENTSO-E Transparency Platform](#). In predicting the national load we selected the following variables.

- Weather temperature;
- Wind speed;
- Hour;
- Month;
- Is holiday: a binary variable for holidays where holiday=1, working day=0;
- Day of week: an ordinal categorical variable corresponding to the day of the week, e.i. Monday=0, ... Sunday=6;

We used the entire 2021 data as the training sample for fitting our models, and we tested them and computed their scores on the 2022 data. The results for Switzerland are reported in Table 1 and figure 2 while results for Germany can be found in Table 2 and figure 3. The error metric used is the pinball loss, scaled by the average load magnitude of each country. It is observed that the KQR model performs marginally better than other QR models and achieves results comparable to those of the GBQR. The superior performance is demonstrated in terms of CRPS to its competitors, quantile regressors, in predicting electricity load quantiles.

Table 1: Pinball loss for load in Switzerland (2022)

Quantile	LQR	GBMQR	QF	KQR
0.1	0.03595	0.01243	0.01479	0.01210
0.2	0.06161	0.01994	0.02200	0.01962
0.3	0.08064	0.02573	0.02743	0.02495
0.4	0.09396	0.02950	0.03073	0.02853
0.5	0.10224	0.03174	0.03218	0.03048
0.6	0.10393	0.03181	0.03115	0.03109
0.7	0.09892	0.03009	0.02807	0.02958
0.8	0.08528	0.02570	0.02293	0.02581
0.9	0.05892	0.01862	0.01487	0.01845
CRPS	0.08016	0.02506	0.02490	0.02451

Table 2: Pinball loss for load in Germany (2022)

Quantile	LQR	GBMQR	QF	KQR
0.1	0.04051	0.02678	0.01585	0.01774
0.2	0.06959	0.03020	0.02431	0.02517
0.3	0.09069	0.03110	0.02852	0.02795
0.4	0.10543	0.03011	0.03089	0.02881
0.5	0.11379	0.02782	0.03200	0.02787
0.6	0.11543	0.02485	0.02993	0.02558
0.7	0.10934	0.02116	0.02610	0.02208
0.8	0.09317	0.01650	0.02120	0.01737
0.9	0.06319	0.01050	0.01264	0.01128
CRPS	0.08901	0.02434	0.02460	0.02265

3.2 SECURES-Met case study

Combining the SECURES-Met data (predictors) [Formayer et al. 2023] and the load data from ENTSOE, we carried out a comparison between different classes of kernels. The kernel functions considered are: Gaussian RBF, Laplacian, Matern 0.5, Matern 1.5, Matern 2.5, linear, periodic, polynomial, sigmoid, and cosine. We used time series cross-validation to evaluate each model's performance, encompassing hyperparameter optimisation and feature selection. In Appendix C, Figure 6 shows the cross-validation process for the Absolute Laplace and Gaussian kernels. The analysis illustrates the criteria and scores to determine the optimal regularisation term and the hyperparameters of the kernel.

Details regarding the hyper-parameter selection for the different kernels can be found in the implementation [here](#). The SECURES-Met data consist of historical data up to the end of 2020 while from 2021 onward, the data consist of forecasts modelled by the European Centre for Medium-Range Weather Forecasts (ECMWF). Therefore, we used the entire data of 2021 as the training set and then tested our kernels on the 2022 data. Note that there are two types of prediction for the data from 2021 onward, one for each of the emission scenarios RCP4.5 and RCP8.5. In this study, we restrict our attention to the RCP4.5 data, since it is part of SURE-SWEET's scenarios.

The predictors making up the dataset follow:

- Direct irradiation: direct normal irradiation.
- Global radiation: mean global radiation.
- Hydro reservoir: daily mean power from reservoir plants in MW.
- Hydro river: daily mean power from run of river plants in MW.
- Temperature: air temperature.
- Wind potential: potential wind power production.

In Appendix C, we have reported the table of quantiles and CRPS scores. Table 7 shows the results for Switzerland, Table 8 for Germany and Table 9 for Austria.

That study provides evidence of the superiority of the Gaussian kernel over the linear and polynomial kernels. In our research, we considered a larger set of kernels. From numerical experiments, the Absolute Laplacian kernel quantile has demonstrated superior performance to other Matern family kernels. In addition, a comprehensive cross-validation process for quantile 0.5 has been conducted to determine optimal hyperparameters and ridge regression parameters to prevent overfitting. The method has also been validated on an extended Secures Met dataset, which includes hydraulic capacity as a variable and technological-economic projections of the energy supply. By including high-resolution hours as a categorical variable, we have achieved accurate predictions and narrower confidence bounds for the Absolute Laplacian and Gaussian RBF Kernels as shown in Figure 8 and Figure 9. The superior performance of the Absolute Laplacian over the Gaussian RBF is largely attributable to the robustness of the Manhattan distance compared to the Euclidean distance [Aggarwal et al. 2001]. The empirical demonstration is provided by comparing the covariance kernels in Figure 7. To complete our analysis, Figures 2 and 3 show a satisfactory prediction and narrow confidence for Switzerland and Germany even when the method slightly fails to approximate the real value.

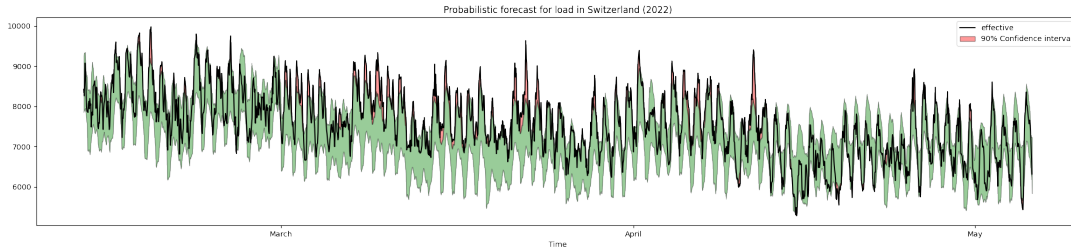


Figure 2: Load 90% confidence interval for Switzerland Energy charts data using KQR Absolute Laplacian: Electric load probabilistic forecast for Switzerland 2022. The black line is the observed path for the load. The 90% confidence interval bands are plotted in green. Lower and upper red lines denote the 95% and 5% quantile forecast respectively.

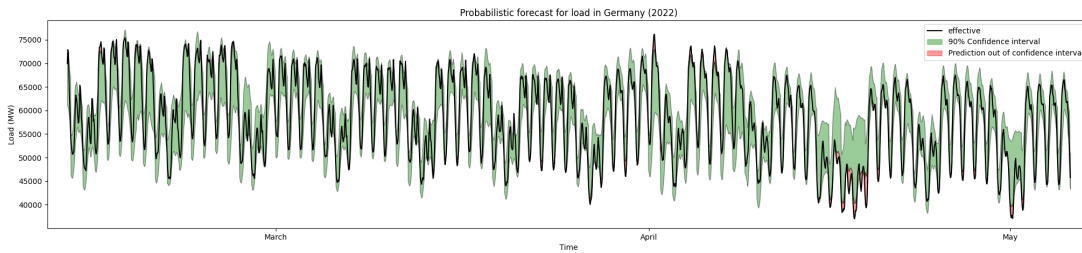


Figure 3: Load 90% confidence interval for Germany Energy charts data using KQR Absolute Laplacian: Electric load probabilistic forecast Germany 2022. The black line is the observed path for the load. The 90% confidence interval bands are plotted in green. Lower and upper red lines denote the 95% and 5% quantile forecast respectively.

4 GEFCom2014 CASE STUDY

We now apply KQR to the setting of probabilistic load and price forecasting. We use the GEFCom2014 [Hong et al. 2014] data to carry out our experiments. The GEFCom is a series of competitions that have been created with the intent of improving forecasting practices, addressing the gap between academia and industry, and fostering state-of-the-art research in the field of energy forecasting [Hong et al. 2016]. The GEFCom edition of 2014 consisted of four tracks, all involving probabilistic forecasting. The four tracks were load, price, wind power, and solar power forecasting. The reason for choosing the GEFCom2014 data is that it is an established benchmark in energy to compare against other valid methods. The data is freely available on Dr. Tao Hong’s [blog](#). Furthermore, a clear comparison can be performed due to the availability of the scores of each method for the load and price track. The score measure of the competition was the pinball loss, see section 2.1, averaged over the 99 quantiles, $q \in \{i/100\}_{i=1}^{99}$. Finally, to recreate the setting of GEFCom2014 and to provide a fair comparison, we adhere rigorously to the rules of the competition. Next, we study the performance of KQR in the load and price tracks. The kernel adopted throughout this study are the [Gaussian RBF](#) and the [Absolute Laplacian kernel](#).

4.1 GEFCom2014 load track

This track was concerned with forecasting hourly loads of an anonymous US utility. The dataset provided at the start of the competition consisted of 69 months of load data and 117 months of weather data, ACM SIGENERGY Energy Informatics Review

both at hourly frequency. In this particular track, the challenge was to predict the load for the next month without the availability of weather temperature forecasts. Therefore, the primary task was to first accurately predict the weather and temperatures and then model the load accordingly. Since there were no attributes available for humidity or wind speed, we chose to predict weather temperatures by aggregating historical temperature data across different dimensions such as day, month, and hour. Then we proceeded with building KQR models for the load; we chose the following predictors.

- Day: the number of the day.
- Hour.
- Day of week: an ordinal categorical variable for the day of the week.
- Is holiday: a dummy variable for holidays.
- w avg: average of weather temperatures across all the 25 stations.

We built 12 models, one for each month, with each task model trained on the historical data of the month associated with it.

Table 3 reports our results for the load track. The top teams for the load forecasting track were Tololo, Adada, Jingrui(Rain) Xie, OxMath, E.S. Managalova, Ziel Florian, and Bidong Liu; for a breakdown of the attributes of each method, see [Hong et al. 2016, Table 6].

We conclude this section with a visualisation of the 90% confidence interval forecast by our model for task number 9, that is the prediction for June, see Figure 4.

The results demonstrate that kernel quantile regression yields scores similar to those of the top five methods outlined in [He et al. 2017], specifically, the method has better performance with respect to non-quantile regression approaches, justifying the selection of this investigation.

4.2 GEFCom2014 price track

In this track, the objective was to forecast electricity prices for the next 24 hours on a rolling basis. The dataset provided consisted of 2.5 years of hourly prices and zonal and system load forecasts. The predictors fed to our KQR models are:

- Day;
- Hour;
- Forecasted total load;
- Forecasted zonal load.

Like above, all models were trained on the historical data of the associated month.

Our results for this track are reported in table 5. In this track, the top entries came from the teams: Tololo, Team Poland, GMD, and C3 Green Team; for a breakdown of each method's attributes, see [Hong et al. 2016, Table 8]. Finally, our probabilistic prediction for the 13th July 2013 zonal price at the 90% confidence interval is visualised in Figure 5.

5 CONCLUSION

In this article, we investigate a non-parametric probabilistic method, the kernel quantile regression, for estimating quantiles of load. To our knowledge, this method has not been explored before for load prediction. We show its effectiveness through several numerical tests on DACH data (Germany, Austria and Switzerland), illustrating that it performs competently compared to other well-known quantile regression techniques and exceeds the point regression results of GEFCom2014. In addition to these numerical experiments, we extend the test case of GEFCom2014 considering additional explanatory variables in hydrocapacity energy storage. We observe that KQR shows favourably and can forecast the medium-term horizon of the Secures-Met dataset. However, the forecasting for the short-term horizon has been demonstrated in the GEFCom2014 price track. The tuning of hyperparameters along with the ridge parameter was carried out using cross-validation, and we presented comprehensive analysis to support the results. In our investigation of kernel functions, we focus on evaluating the Absolute Laplace kernel in comparison to the RBF Gaussian Kernel during the kernel selection procedure. The results of this study confirm the durability of our selection in terms of precision of prediction. Finally, we provide an open-source implementation of KQR integrated with the most popular tools in the community. This investigation will serve as a case study for an uncertainty quantification model to predict the impact of climate shocks on pathways, which will be further refined in scenarios computed by the SURE SWEET energy models. Further investigation with different choices and combinations of kernels as well as a detailed comparison with gradient booster methods remains a future research area.

ACM SIGENERGY Energy Informatics Review

6 ACKNOWLEDGMENTS

We are grateful to three anonymous reviewers for insightful feedback. We are thankful for the fruitful discussions with Michael Multerer and Paul Schneider. Davide Baroli and Luca Pernigo carried out this research with the support of the Swiss Federal Office of Energy SFOE as part of the SWEET project SURE. The authors bear sole responsibility for the conclusions and the results presented in this publication. Rohan Sen was supported by the SNF grant "Scenarios" (100018_189086).

REFERENCES

- Farzaneh Abbaspourtorbati and Marek Zima. 2016. The Swiss Reserve Market: Stochastic Programming in Practice. *IEEE Transactions on Power Systems* 31, 2 (March 2016), 1188–1194.
- Charu C. Aggarwal, Alexander Hinneburg, and Daniel A. Keim. 2001. On the Surprising Behavior of Distance Metrics in High Dimensional Space. In Proceedings of the 8th International Conference on Database Theory. *Lecture Notes in Computer Science* 1, 1, 420–434. https://doi.org/10.1007/3-540-44503-x_27
- Nachman Aronszajn. 1950. Theory of reproducing kernels. *Transactions of the American mathematical society* 68, 3 (1950), 337–404.
- Alain Berlinet and Christine Thomas-Agnan. 2011. *Reproducing kernel Hilbert spaces in probability and statistics*. Springer Science & Business Media, NY, USA.
- Stephen P Boyd and Lieven Vandenbergh. 2004. *Convex optimization*. Cambridge University Press, Cambridge, UK.
- Laurent Dubus, Yves-Marie Saint-Drenan, Alberto Troccoli, Matteo De Felice, Yohann Moreau, Linh Ho-Tran, Clare Goodess, Rodrigo Amaro e Silva, and Luke Sanger. 2023. C3SEnergy: A climate service for the provision of power supply and demand indicators for Europe based on the ERA5 reanalysis and ENTSO-E data.
- Herbert Formayer, Imran Nadeem, David Leidinger, Philipp Maier, Franziska Schöniger, Demet Suna, Gustav Resch, Gerhard Totschnig, and Fabian Lehner. 2023. SECURES-Met: A European meteorological data set suitable for electricity modelling applications. *Scientific Data* 10, 1 (2023). <https://doi.org/10.1038/s41597-023-02494-4>
- Tilmann Gneiting. 2011. Quantiles as optimal point forecasts. *International Journal of Forecasting* 27, 2 (2011), 197–207.
- Tilmann Gneiting, Fadoua Balabdaoui, and Adrian E Raftery. 2007. Probabilistic Forecasts, Calibration and Sharpness. , 243–268 pages.
- Tilmann Gneiting, Sebastian Lerch, and Benedikt Schulz. 2023. Probabilistic solar forecasting: Benchmarks, post-processing, verification. *Solar Energy* 252 (2023), 72–80.
- Yaoyao He and Haiyan Li. 2018. Probability density forecasting of wind power using quantile regression neural network and kernel density estimation. *Energy conversion and management* 164 (2018), 374–384.
- Yaoyao He, Rui Liu, Haiyan Li, Shuo Wang, and Xiaofen Lu. 2017. Short-term power load probability density forecasting method using kernel-based support vector quantile regression and Copula theory. *Applied energy* 185 (2017), 254–266.
- Linh Ho-Tran and Stephanie Fiedler. 2024. A climatology of weather-driven anomalies in European photovoltaic and wind power production.
- Tao Hong and Shu Fan. 2016. Probabilistic electric load forecasting: A tutorial review. *International Journal of Forecasting* 32, 3 (2016), 914–938.
- Tao Hong, Pierre Pinson, and Shu Fan. 2014. Global energy forecasting competition 2012. , 357–363 pages.
- Tao Hong, Pierre Pinson, Shu Fan, Hamidreza Zareipour, Alberto Troccoli, and Rob J Hyndman. 2016. Probabilistic electric load forecasting: Global energy forecasting competition 2014 and beyond. , 896–913 pages.
- Changha Hwang and Jooyong Shim. 2005. A Simple Quantile Regression via Support Vector Machine. , 512–520 pages.
- Ramachandran Kannan. 2018. Dynamics of long-term electricity demand profile: Insights from the analysis of Swiss energy systems. *Energy Strategy Reviews* 22 (Nov. 2018), 410–425. <https://doi.org/10.1016/j.esr.2018.10.010>
- Ramachandran Kannan, Evangelos Panos, Stefan Hirschberg, and Tom Kober. 2022. A net-zero Swiss energy system by 2050: Technological and policy options for the transition of the transportation sector. *FUTURES; FORESIGHT SCIENCE* 4, 3–4 (March 2022), 126–148. <https://doi.org/10.1002/flo2.126>
- Roger Koenker. 2005. *Quantile Regression*. Vol. 38. Cambridge University Press, Cambridge, UK.
- Roger Koenker and Gilbert Bassett Jr. 1978. Regression quantiles. *Econometrica: journal of the Econometric Society* 46, 1 (1978), 33–50.
- Roger Koenker and Kevin F. Hallock. 2001. Quantile Regression. *The Journal of Economic Perspectives* 15, 4 (2001), 143–156. <http://www.jstor.org/stable/2696522>
- Jesus Lago, Grzegorz Marcjasz, Bart De Schutter, and Rafal Weron. 2021. Forecasting day-ahead electricity prices: A review of state-of-the-art algorithms, best practices and an open-access benchmark. *Applied Energy* 293 (2021), 116983.

Volume 4 Issue 4, October 2024

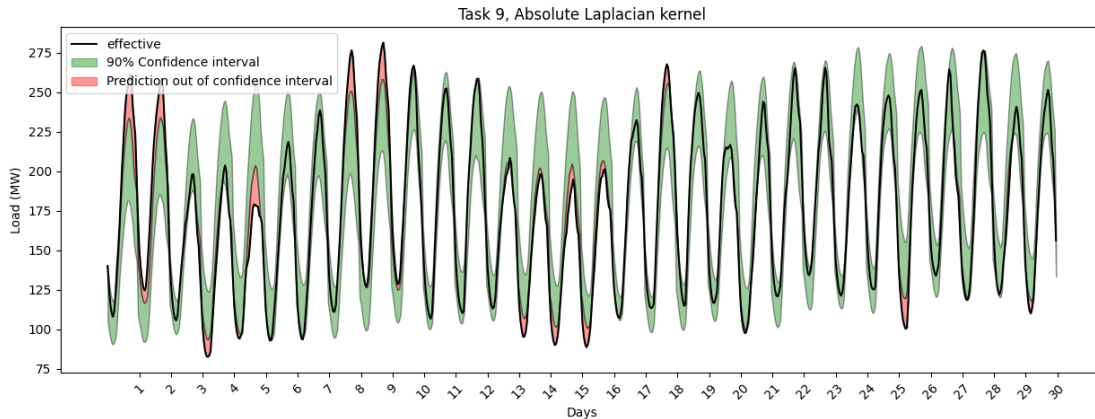


Figure 4: Load 90% confidence interval task 9 using KQR Absolute Laplacian: Electric load probabilistic forecast for June 2011. The black line is the observed path for the load. The 90% confidence interval bands are plotted in green. Lower and upper red lines denote the 95% and 5% quantile forecast respectively. The prediction out-of confidence interval is denoted in red.

Table 3: Pinball loss GEFCom2014 load data

Team name\Task number	1	2	3	4	5	6	7	8	9	10	11	12
KQR Absolute Laplacian	12.5357	11.0209	9.4492	5.2240	6.6145	6.5418	11.2004	11.6325	5.9476	5.2219	7.5478	11.0587
KQR Gaussian RBF	12.4660	11.0894	9.4938	5.1826	6.9575	6.7947	10.8825	11.5542	5.9742	5.0779	7.3797	10.3110
Adada	10.5093	10.0801	7.6238	4.7289	5.3936	6.6242	8.0144	11.1366	5.7779	3.6379	7.0096	8.9109
Benchmark - Load	18.7384	22.7585	13.2163	8.3626	10.9162	16.9937	13.4038	17.3151	13.8374	6.4237	10.9380	34.0685
C3 Green Team	18.7384	19.2208	7.9637	4.6370	6.4543	8.3799	10.5546	10.6609	5.8867	4.4866	5.9396	10.3917
E.S. Mangalova	18.7384	13.3340	7.8025	4.4096	6.6330	6.2306	10.1511	10.9294	6.2224	4.2382	6.5464	8.8080
Jingrui (Rain) Xie	11.8700	10.9250	8.4938	4.9611	7.4442	6.9921	9.0523	11.2600	5.4864	3.3602	5.9011	9.7316
OxMath	14.4091	8.9136	7.6059	4.4548	7.2944	7.4551	7.9527	10.2444	5.4551	4.2111	6.4054	9.5520
Tololo	10.4369	12.5232	8.2695	4.4220	5.8976	6.1878	7.3182	10.8032	5.4469	3.9613	6.3173	8.4787

Table 4: GEFCom2014 load data ranking

Team name\Task number	1	2	3	4	5	6	7	8	9	10	11	12	Aggregate ranking
KQR Absolute Laplacian	6/362	7/362	14/362	10/362	4/362	3/362	20/362	15/362	9/362	16/362	18/362	12/362	11/362
KQR Gaussian RBF	5/362	8/362	15/362	9/362	8/362	7/362	18/362	12/362	10/362	15/362	17/362	8/362	10/362

Table 5: Pinball loss GEFCom2014 price data

Team name\Task number	1	2	3	4	5	6	7	8	9	10	11	12
KQR Absolute Laplacian	1.02492	3.35057	4.21374	7.33987	5.00981	6.96522	3.57168	1.77610	1.28765	2.73863	2.39831	23.30234
KQR Gaussian RBF	1.84673	2.81882	1.54608	8.31636	4.05988	6.60456	3.57818	2.02177	1.45779	2.20701	1.98184	21.41033
Benchmark - Price	4,02875	7,97208	5,70395	12,15104	38,33541	44,22979	18,22395	31,56729	42,94958	2,85583	3,20395	22,38333
C3 Green Team	1,85897	3,27786	1,2593	5,08886	6,87674	6,1505	4,42379	1,32639	1,25915	3,08224	1,55811	6,58123
GMD	3,7271	1,783	0,92191	5,08886	6,21331	3,82599	4,9342	1,47858	1,65933	2,06134	2,1235	6,84571
Team Poland	1,97477	1,81898	1,19162	2,82318	7,55914	4,20773	2,59715	1,04693	1,24193	4,06012	1,08458	3,06512
Tololo	1,70734	1,45173	1,10384	2,01694	9,15596	4,6821	1,59517	0,75352	2,45935	2,9614	1,34614	3,55819
pat1	2,36615	1,98567	1,07248	2,79465	4,23269	4,70614	8,40506	1,25376	2,23991	3,67952	1,06139	6,27517

Youjuan Li, Yufeng Liu, and Ji Zhu. 2007. Quantile Regression in Reproducing Kernel Hilbert Spaces. *J. Amer. Statist. Assoc.* 102, 477 (2007), 255–268.

Sandro Luh, Ramachandran Kannan, Russell McKenna, Thomas J Schmidt, and Tom Kober. 2023. How, where, and when to charge electric vehicles – net-zero energy system implications and policy recommendations. *Environmental Research*

Communications 5, 9 (Sept. 2023), 095004. <https://doi.org/10.1088/2515-7620/acf363>

Rui Moreira, Ricardo Bessa, and Joao Gama. 2016. Probabilistic forecasting of day-ahead electricity prices for the Iberian electricity market. In *2016 13th International Conference on the European Energy Market (EEM)*. IEEE, NY, 1–5.

Table 6: GEFCom2014 price data ranking

Team name\Task number	1	2	3	4	5	6	7	8	9	10	11	12	Aggregate ranking
KQR Absolute Laplacian	1/287	11/287	12/287	14/287	4/287	11/287	5/287	8/287	6/287	8/287	15/287	18/287	15/287
KQR Gaussian RBF	6/287	8/287	10/287	15/287	1/287	10/287	6/287	10/287	7/287	5/287	9/287	16/287	10/287

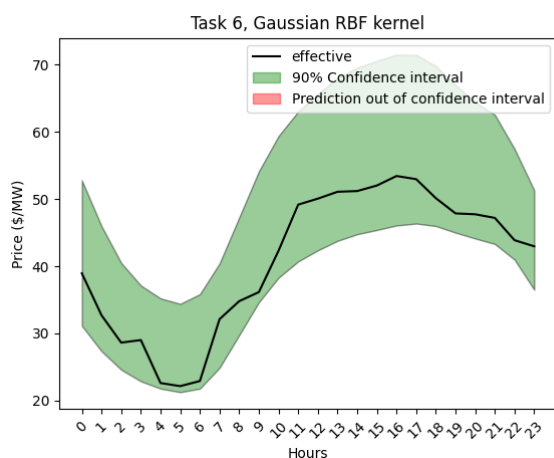


Figure 5: Price 90% confidence interval task 6: Electricity price probabilistic forecast for the 13th July 2013. The black line is the observed path for the price. The 90% confidence interval bands are plotted in green. Lower and upper red lines denote the 95% and 5% quantile forecast respectively.

Claudio Nägeli, Martin Jakob, Giacomo Catenazzi, and York Ostermeyer. 2020. Towards agent-based building stock modeling: Bottom-up modeling of long-term stock dynamics affecting the energy and climate impact of building stocks. *Energy and Buildings* 211 (March 2020), 109763. <https://doi.org/10.1016/j.enbuild.2020.109763>

Jakub Nowotarski and Rafal Weron. 2018a. Recent advances in electricity price forecasting: A review of probabilistic forecasting. *Renewable and Sustainable Energy Reviews* 81 (2018), 1548–1568.

Jakub Nowotarski and Rafal Weron. 2018b. Recent advances in electricity price forecasting: A review of probabilistic forecasting. *Renewable and Sustainable Energy Reviews* 81 (2018), 1548–1568.

Evangelos Panos, Ramachandran Kannan, Stefan Hirschberg, and Tom Kober. 2023. An assessment of energy system transformation pathways to achieve net-zero carbon dioxide emissions in Switzerland. *Communications Earth; Environment* 4, 1 (2023), 157–170. <https://doi.org/10.1038/s43247-023-00813-6>

Fabian Pedregosa, Gaël Varoquaux, Alexandre Gramfort, Vincent Michel, Bertrand Thirion, Olivier Grisel, Mathieu Blondel, Peter Prettenhofer, Ron Weiss, Vincent Dubourg, Jake Vanderplas, Alexandre Passos, David Cournapeau, Matthieu Brucher, Matthieu Perrot, and Édouard Duchesnay. 2011. Scikit-learn: Machine Learning in Python. *Journal of Machine Learning Research* 12, 85 (2011), 2825–2830.

Kaleb Phipps, Stefan Meisenbacher, Benedikt Heidrich, Marian Turowski, Ralf Mikut, and Veit Hagemeyer. 2023. Loss-Customised Probabilistic Energy Time Series Forecasts Using Automated Hyperparameter Optimisation. <https://doi.org/10.1145/3575813.3595204>

Maxime Sangnier, Olivier Fercoq, and Florence d’Alché-Buc. 2016. Joint quantile regression in vector-valued RKHSs. , 3700–3708 pages.

Bernhard Schölkopf, Ralf Herbrich, and Alex J. Smola. 2001. A Generalized Representer Theorem. In *Computational Learning Theory*, David Helmbold and Bob Williamson (Eds.). Springer Berlin Heidelberg, Berlin, Heidelberg, 416–426.

Bernhard Schölkopf and Alexander J. Smola. 2018. *Learning with Kernels: Support Vector Machines, Regularization, Optimization, and Beyond*. The MIT Press, Cambridge, MA.

Ichiro Takeuchi, Quoc V. Le, Timothy D. Sears, and Alexander J. Smola. 2006. Non-parametric Quantile Estimation. *Journal of Machine Learning Research* 7, 45 (2006), 1231–1264.

Evelina Trutnevte. 2013. EXPANSE methodology for evaluating the economic potential of renewable energy from an energy mix perspective. *Applied Energy* 111 (Nov. 2013), 593–601. <https://doi.org/10.1016/j.apenergy.2013.04.083>

Dennis W Van der Meer, Joakim Widén, and Joakim Munkhammar. 2018. Review on probabilistic forecasting of photovoltaic power production and electricity consumption. *Renewable and Sustainable Energy Reviews* 81 (2018), 1484–1512.

Lieven Vandenberghe. 2010. The CVXOPT linear and quadratic cone program solvers. Vladimir N. Vapnik. 1997. The support vector method. In *Artificial Neural Networks – ICANN’97*. Springer Berlin Heidelberg, Berlin, Heidelberg, 261–271.

Qifa Xu, Jinxiu Zhang, Cuixia Jiang, Xue Huang, and Yaoyao He. 2015. Weighted quantile regression via support vector machine. *Expert Systems with Applications* 42, 13 (2015), 5441–5451.

Chong Zhang, Yufeng Liu, and Yichao Wu. 2016. On Quantile Regression in Reproducing Kernel Hilbert Spaces with the Data Sparsity Constraint. *Journal of Machine Learning Research* 17, 40 (2016), 1–45.

Songfeng Zheng. 2021. Fast quantile regression in reproducing kernel Hilbert space. *Journal of the Korean Statistical Society* 51, 2 (Oct. 2021), 568–588.

Florian Ziel and Rick Steinert. 2018. Probabilistic mid-and long-term electricity price forecasting. *Renewable and Sustainable Energy Reviews* 94 (2018), 251–266.

Nik Zielonka, Xin Wen, and Evelina Trutnevte. 2023. Probabilistic projections of granular energy technology diffusion at subnational level.

A PINBALL LOSS FUNCTION FOR QUANTILE REGRESSION

In this section, we show why minimizing the pinball loss function leads to estimates of the quantile. This section has been sourced from [Koenker 2005] and hence, we would like to refer to the above reference for further details on the same. For a real-valued random variable X with distribution function $F(\cdot)$, the q -th quantile is defined as

$$Q(q) := \inf \{x \in \mathbb{R} : F(x) \geq q\} \quad \text{for } 0 \leq q \leq 1. \quad (\text{A.1})$$

For a continuous distribution function $F(\cdot)$, the quantile becomes just the inverse, i.e. $Q = F^{-1}$. For example, $q = 0.5$ defines the median of the distribution of X . The quantiles arise from a simple optimization problem that is fundamental to all that follows. Consider a simple decision-theoretic problem: a point estimate is required for a random variable with (posterior) distribution function F . If the loss is described by the piecewise linear pinball loss, cp. (2.1), consider the problem of finding \hat{x} to minimize the expected loss. We seek to minimize

$$\begin{aligned} \mathbb{E} [\rho_q(X - \hat{x})] &= q \int_{\hat{x}}^{\infty} (x - \hat{x}) dF(x) \\ &\quad - (1 - q) \int_{-\infty}^{\hat{x}} (x - \hat{x}) dF(x). \end{aligned} \quad (\text{A.2})$$

To find the optimal \hat{x} , we consider the first-order conditions by differentiating problem A.2 with respect to \hat{x} and setting it to zero:

$$0 = -q \int_{\hat{x}}^{\infty} dF(x) + (1 - q) \int_{-\infty}^{\hat{x}} dF(x) = F(\hat{x}) - q$$

Since $F(\cdot)$ is a monotone function, any element of $\{x : F(x) = q\}$ minimizes expected loss. When the solution is unique, $\hat{x} = F^{-1}(q)$, otherwise, we have an “interval of q quantiles” from which the smallest element must be chosen - to adhere to the convention that the empirical quantile function be left-continuous. When $F(\cdot)$ is

replaced by the empirical distribution function

$$F_n(x) = \frac{1}{n} \sum_{i=1}^n \mathbb{I}\{X_i \leq x\}, \quad (\text{A.3})$$

we may still choose \hat{x} to minimize expected loss:

$$\int_{\mathbb{R}} \rho_q(x - \hat{x}) dF_n(x) = \frac{1}{n} \sum_{i=1}^n \rho_q(x_i - \hat{x}) \quad (\text{A.4})$$

where x_i 's are now assumed to be generated from the independently and identically distributed random variables $X_i \sim F(\cdot)$; doing so now yields the q -th sample quantile. When qn is an integer there is again some ambiguity in the solution, because we really have an interval of solutions, $\{x : F_n(x) = q\}$, but this is of little practical consequence.

B ESTIMATOR DERIVATION FOR KERNEL QUANTILE REGRESSION

The goal is to solve the optimization problem, cp. (2.8)

$$\operatorname{argmin}_{w \in \mathcal{H}, b \in \mathbb{R}} C \sum_{i=1}^n \rho_q(y_i - (\langle w, \phi(x_i) \rangle_{\mathcal{H}} + b)) + \frac{1}{2} \|w\|_{\mathcal{H}}^2, \quad (\text{B.1})$$

with the characterization $f(x) = \langle w, \phi(x) \rangle_{\mathcal{H}} + b$. Minimizing $\|w\|_{\mathcal{H}}^2$ is equivalent to minimizing the regularizer, see [Schölkopf and Smola 2018, Section 2.2.4]. Using the definition of the pinball loss function, cp. (2.1), we have the problem

$$\operatorname{argmin}_{w \in \mathcal{H}, b \in \mathbb{R}} C \sum_{i=1}^n q(y_i - \langle w, \phi(x_i) \rangle_{\mathcal{H}} - b) + (1-q)(-y_i + \langle w, \phi(x_i) \rangle_{\mathcal{H}} + b) + \frac{1}{2} \|w\|_{\mathcal{H}}^2, \quad (\text{B.2})$$

Introducing the slack variables ξ_i, ξ_i^* , $1 \leq i \leq n$, we can rephrase Problem B.2 as the following constrained optimization problem, see [Hwang and Shim 2005; Takeuchi et al. 2006]

$$\begin{aligned} \operatorname{argmin}_{w \in \mathcal{H}, b, \xi_i, \xi_i^* \in \mathbb{R}} & C \sum_{i=1}^n q \xi_i + (1-q) \xi_i^* + \frac{1}{2} \|w\|_{\mathcal{H}}^2 \\ \text{s.t.} & y_i - \langle w, \phi(x_i) \rangle_{\mathcal{H}} - b \leq \xi_i, \\ & -y_i + \langle w, \phi(x_i) \rangle_{\mathcal{H}} + b \leq \xi_i^*, \\ & \xi_i \geq 0, \quad \xi_i^* \geq 0. \end{aligned} \quad (\text{B.3})$$

Now, by the representer theorem, see [Schölkopf et al. 2001], any $w \in \mathcal{H}$ that minimizes Problem B.1 can be written as

$$w = \sum_{i=1}^n a_i \phi(x_i) \implies w(x) = \sum_{i=1}^n a_i \mathcal{K}(x, x_i).$$

Using (2.5), we have that $\langle w, \phi(x_j) \rangle_{\mathcal{H}} = w(x_j) = \sum_{i=1}^n a_i \mathcal{K}(x_i, x_j)$ for $1 \leq j \leq n$. Hence, denoting the coefficient vector as $\mathbf{a} := [a_i]_{i=1}^n \in \mathbb{R}^n$, we have that

$$[\langle w, \phi(x_j) \rangle_{\mathcal{H}}]_{j=1}^n = \mathbf{K} \mathbf{a}, \quad \|w\|_{\mathcal{H}}^2 = \mathbf{a}^\top \mathbf{K} \mathbf{a}. \quad (\text{B.4})$$

Using the notations $\mathbf{y} := [y_i]_{i=1}^n \in \mathbb{R}^n$, $\boldsymbol{\xi} := [\xi_i]_{i=1}^n \in \mathbb{R}^n$, $\boldsymbol{\xi}^* := [\xi_i^*]_{i=1}^n \in \mathbb{R}^n$, we have the equivalent problem in matrix notation

$$\begin{aligned} \operatorname{argmin}_{\mathbf{a}, \boldsymbol{\xi}, \boldsymbol{\xi}^* \in \mathbb{R}^n, b \in \mathbb{R}} & Cq \boldsymbol{\xi}^\top \mathbf{1} + C(1-q)(\boldsymbol{\xi}^*)^\top \mathbf{1} + \frac{1}{2} \mathbf{a}^\top \mathbf{K} \mathbf{a} \\ \text{s.t.} & \mathbf{y} - \mathbf{K} \mathbf{a} - b \mathbf{1} \leq \boldsymbol{\xi}, \\ & -\mathbf{y} + \mathbf{K} \mathbf{a} + b \mathbf{1} \leq \boldsymbol{\xi}^*, \\ & \boldsymbol{\xi} \geq \mathbf{0}, \quad \boldsymbol{\xi}^* \geq \mathbf{0}. \end{aligned} \quad (\text{B.5})$$

Through the Lagrange multipliers and the KKT conditions (see [Boyd and Vandenberghe 2004]), Problem B.5 can be solved to its equivalent dual formulation, see [Takeuchi et al. 2006; Xu et al. 2015] for more details. We can write the Lagrangian as

$$\begin{aligned} L(\mathbf{a}, b, \boldsymbol{\xi}, \boldsymbol{\xi}^*, \boldsymbol{\alpha}, \boldsymbol{\alpha}^*, \mathbf{v}, \mathbf{v}^*) & := Cq \boldsymbol{\xi}^\top \mathbf{1} + C(1-q)(\boldsymbol{\xi}^*)^\top \mathbf{1} + \frac{1}{2} \mathbf{a}^\top \mathbf{K} \mathbf{a} \\ & - \boldsymbol{\alpha}^\top (\boldsymbol{\xi} - \mathbf{y} + \mathbf{K} \mathbf{a} + b \mathbf{1}) - (\boldsymbol{\alpha}^*)^\top (\boldsymbol{\xi}^* + \mathbf{y} - \mathbf{K} \mathbf{a} - b \mathbf{1}) \\ & - \mathbf{v}^\top \boldsymbol{\xi} - (\mathbf{v}^*)^\top \boldsymbol{\xi}^*, \end{aligned} \quad (\text{B.6})$$

with the positivity constraints $\boldsymbol{\alpha}, \boldsymbol{\alpha}^*, \mathbf{v}, \mathbf{v}^* \geq \mathbf{0}$. We proceed to derive the dual function by minimizing the Lagrangian

$$g(\boldsymbol{\alpha}, \boldsymbol{\alpha}^*, \mathbf{v}, \mathbf{v}^*) = \inf_{\mathbf{a}, \boldsymbol{\xi}, \boldsymbol{\xi}^* \in \mathbb{R}^n, b \in \mathbb{R}} L(\mathbf{a}, \boldsymbol{\xi}, \boldsymbol{\xi}^*, \boldsymbol{\alpha}, \boldsymbol{\alpha}^*, \mathbf{v}, \mathbf{v}^*). \quad (\text{B.7})$$

Setting the partial derivatives to zero, we have

$$\begin{cases} \frac{\partial L}{\partial \mathbf{a}} = \mathbf{0} \implies \mathbf{K} \mathbf{a} = \mathbf{K}(\boldsymbol{\alpha} - \boldsymbol{\alpha}^*), \\ \frac{\partial L}{\partial b} = \mathbf{0} \implies (\boldsymbol{\alpha} - \boldsymbol{\alpha}^*)^\top \mathbf{1} = 0, \\ \frac{\partial L}{\partial \boldsymbol{\xi}} = \mathbf{0} \implies Cq \mathbf{1} = \boldsymbol{\alpha} + \mathbf{v}, \\ \frac{\partial L}{\partial \boldsymbol{\xi}^*} = \mathbf{0} \implies C(1-q) \mathbf{1} = \boldsymbol{\alpha}^* + \mathbf{v}^*. \end{cases} \quad (\text{B.8})$$

Substituting the conditions into B.6, we obtain the dual function as

$$\begin{aligned} g(\boldsymbol{\alpha}, \boldsymbol{\alpha}^*, \mathbf{v}, \mathbf{v}^*) & = -\frac{1}{2} (\boldsymbol{\alpha} - \boldsymbol{\alpha}^*)^\top \mathbf{K} (\boldsymbol{\alpha} - \boldsymbol{\alpha}^*) + (\boldsymbol{\alpha} - \boldsymbol{\alpha}^*)^\top \mathbf{y}, \\ \text{s.t.} & (\boldsymbol{\alpha} - \boldsymbol{\alpha}^*) = \mathbf{a}, \\ & (\boldsymbol{\alpha} - \boldsymbol{\alpha}^*)^\top \mathbf{1} = 0, \\ & \mathbf{0} \leq \boldsymbol{\alpha} \leq Cq, \\ & \mathbf{0} \leq \boldsymbol{\alpha}^* \leq C(1-q). \end{aligned} \quad (\text{B.9})$$

In terms of the coefficient vector \mathbf{a} , we can consider the dual optimization problem which turns out to be (after switching signs)

$$\begin{aligned} \operatorname{argmin}_{\mathbf{a} \in \mathbb{R}^n} & +\frac{1}{2} \mathbf{a}^\top \mathbf{K} \mathbf{a} - \mathbf{a}^\top \mathbf{y} \\ \text{s.t.} & C(q-1) \mathbf{1} \leq \mathbf{a} \leq Cq \mathbf{1} \\ & \mathbf{a}^\top \mathbf{1} = 0. \end{aligned} \quad (\text{B.10})$$

From the constraint conditions of problem B.9 and the expression of w cp. (2.9), we have that the optimal w is given by the coefficients

$$w = \sum_{i=1}^n a_i^* \phi(x_i), \quad (\text{B.11})$$

where $\mathbf{a}^* = [a_i^*]_{i=1}^n$ is the solution of Problem B.10. Finally, the data points for which $a_i^* \notin \{C(q-1), Cq\}$ are called the support vectors. The intercept term b can be calculated using the fact that $f(x_i) = y_i$ for the set of support vectors, see [Takeuchi et al. 2006; Xu et al. 2015] for more details. The latter holds due to KKT conditions on Problem B.10.

C ADDITIONAL NUMERICAL COMPARISONS

In this Appendix, we present additional investigations that demonstrate the reliability and robustness of the KQR method introduced in the GECom2014 and Secures MET case study.

Table 7: Pinball loss for load in Switzerland case study with SECURES-Met dataset

Quantile	Absolute Laplacian	Matern 0.5/ Laplacian	Matern 1.5	Matern 2.5	Matern ∞ / Gaussian RBF	Linear	Periodic	Polynomial	Sigmoid	Cosine
0.1	0.018783	0.018988	0.019108	0.019257	0.019547	0.019952	0.018891	0.019654	0.021456	0.021921
0.2	0.030441	0.030668	0.030809	0.031028	0.031546	0.032158	0.030683	0.031857	0.034032	0.034629
0.3	0.038467	0.038864	0.039050	0.039285	0.039907	0.040657	0.038968	0.040075	0.042944	0.043393
0.4	0.043622	0.044186	0.044516	0.044706	0.045286	0.046153	0.044354	0.045506	0.048701	0.048977
0.5	0.046160	0.046792	0.047205	0.047450	0.048116	0.048951	0.046956	0.047891	0.051423	0.051896
0.6	0.045499	0.046133	0.046824	0.047177	0.047840	0.048667	0.046446	0.047496	0.051292	0.051894
0.7	0.041494	0.042044	0.042928	0.043371	0.044104	0.044926	0.042458	0.043565	0.047656	0.048275
0.8	0.033837	0.034128	0.034797	0.035325	0.036166	0.037055	0.034290	0.035533	0.039501	0.040007
0.9	0.021883	0.021871	0.022431	0.022682	0.023169	0.023730	0.022000	0.022811	0.025561	0.026019
CRPS	0.035576	0.035964	0.036407	0.036698	0.037298	0.038028	0.036116	0.037154	0.040285	0.040779

Table 8: Pinball loss for load in German case study with SECURES-Met dataset

Quantile	Absolute Laplacian	Matern 0.5/ Laplacian	Matern 1.5	Matern 2.5	Matern ∞ / Gaussian RBF	Linear	Periodic	Polynomial	Sigmoid	Cosine
0.1	0.025734	0.026272	0.026642	0.026845	0.027090	0.027306	0.026139	0.026621	0.027954	0.028004
0.2	0.043114	0.044138	0.044733	0.045057	0.045469	0.045917	0.044088	0.044716	0.046925	0.047025
0.3	0.054861	0.056343	0.056930	0.057335	0.057920	0.058528	0.056229	0.057066	0.060092	0.060209
0.4	0.061436	0.063490	0.064291	0.064748	0.065433	0.066136	0.063324	0.064683	0.067979	0.068202
0.5	0.064144	0.066330	0.067229	0.067696	0.068275	0.068960	0.066325	0.071421	0.070957	0.071359
0.6	0.062306	0.064676	0.065836	0.066299	0.066881	0.067405	0.064660	0.069160	0.068494	0.068780
0.7	0.055491	0.057851	0.058848	0.059317	0.059878	0.060275	0.061442	0.061423	0.060988	0.060990
0.8	0.044023	0.045011	0.045441	0.045644	0.046008	0.046374	0.047348	0.047182	0.047071	0.047056
0.9	0.026178	0.026126	0.026160	0.026187	0.026207	0.026282	0.026772	0.026766	0.026581	0.026628
CRPS	0.048587	0.050026	0.050679	0.051014	0.051462	0.051909	0.050703	0.052115	0.053005	0.053139

Table 9: Pinball loss for load in Austrian case study with SECURES-Met dataset

Quantile	Absolute Laplacian	Matern 0.5/ Laplacian	Matern 1.5	Matern 2.5	Matern ∞ / Gaussian RBF	Linear	Periodic	Polynomial	Sigmoid	Cosine
0.1	0.024365	0.024592	0.024550	0.024611	0.024831	0.026853	0.025744	0.026004	0.027672	0.027816
0.2	0.040971	0.041406	0.041413	0.041487	0.041857	0.045007	0.043247	0.043720	0.045899	0.045879
0.3	0.052316	0.052969	0.052888	0.052973	0.053449	0.057880	0.055231	0.055446	0.058572	0.058454
0.4	0.058286	0.059018	0.058916	0.059078	0.059592	0.065770	0.061844	0.062495	0.066599	0.066335
0.5	0.060344	0.061100	0.061319	0.061541	0.062338	0.068197	0.063864	0.071731	0.069761	0.069574
0.6	0.058724	0.059507	0.059674	0.059930	0.060709	0.065828	0.062265	0.070269	0.067179	0.066970
0.7	0.053148	0.054189	0.054249	0.054372	0.054916	0.058548	0.055830	0.063015	0.059807	0.059419
0.8	0.042740	0.043368	0.043408	0.043510	0.043881	0.046017	0.044384	0.049813	0.047078	0.046662
0.9	0.026430	0.026583	0.026781	0.026817	0.026908	0.027050	0.026471	0.030279	0.028031	0.027986
CRPS	0.046369	0.046970	0.047022	0.047146	0.047609	0.051239	0.048764	0.052530	0.052289	0.052122

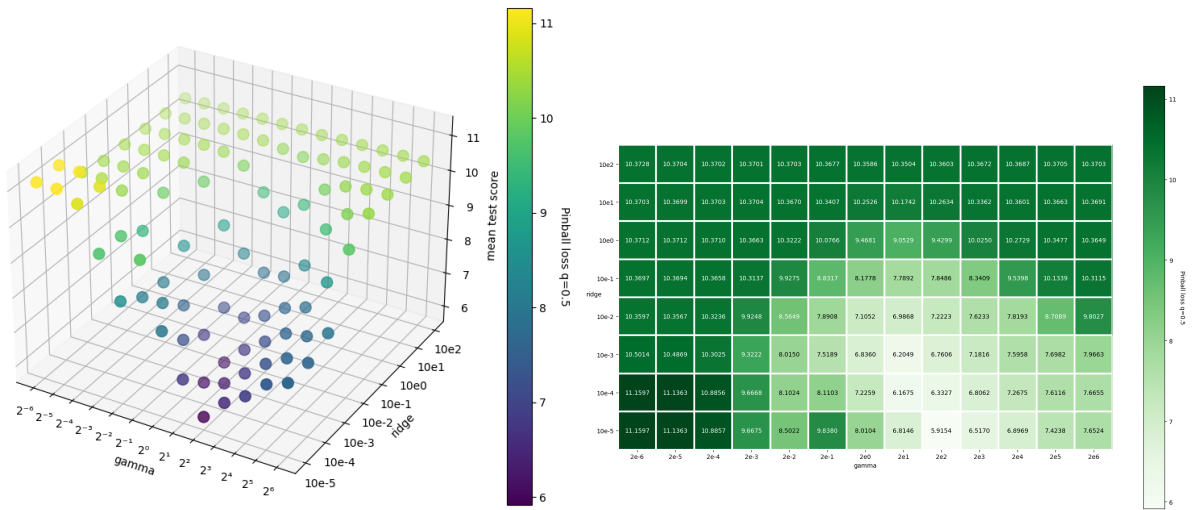


Figure 6: Hyperparameter cross-validation for the RBF Kernel Quantile Method applied to the price task 4, specifically the cross-validation is obtained for the median quantile. On the left, the figure illustrates the optimal hyperparameters selection based on the mean quantile score. The same result is presented using a heatmap.

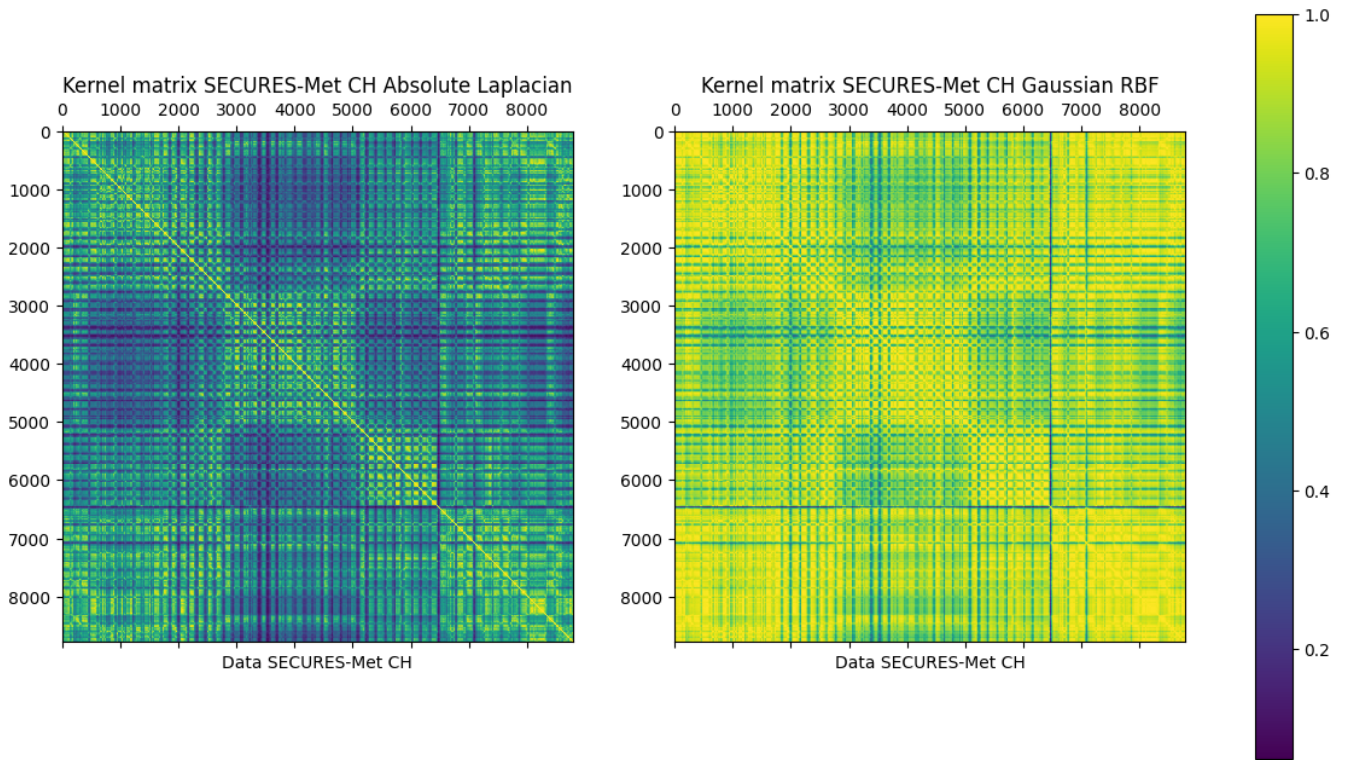


Figure 7: Comparison between the kernel covariance evaluation for Absolute Laplacian and Gaussian RBF kernel for SECURE-Met study.

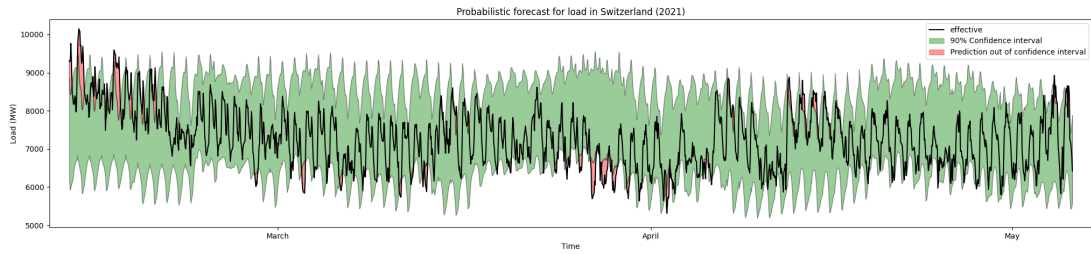


Figure 8: Prediction and confidence bound of Absolute Laplacian kernel in Secures MET study. The black line is the observed path for the load. The 90% confidence interval bands are plotted in green. Lower and upper red lines denote the 95% and 5% quantile forecast respectively. The prediction out-of confidence interval is denoted in red.

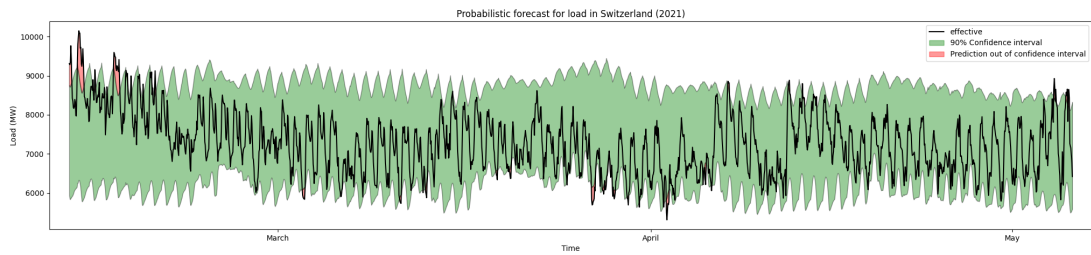


Figure 9: Prediction and confidence bound of Gaussian RBF kernel in Secures MET study. The black line is the observed path for the load. The 90% confidence interval bands are plotted in green. Lower and upper red lines denote the 95% and 5% quantile forecast respectively. The prediction out-of confidence interval is denoted in red.